

Adiabatic magnetization of superconductors as a high-performance cooling mechanism

Fabrizio Dolcini*

*NEST CNR-INFM and Scuola Normale Superiore, I-56126 Pisa, Italy
and Dipartimento di Fisica del Politecnico di Torino, I-10129 Torino, Italy*

Francesco Giazotto†

NEST CNR-INFM and Scuola Normale Superiore, I-56126 Pisa, Italy

(Received 8 June 2009; published 6 July 2009)

The adiabatic magnetization of a superconductor is a cooling principle proposed in the 1930s, which has remained mostly unexploited so far. Here we present a detailed dynamic description of the effect, computing the achievable final temperatures as well as the process time scales for different superconductors in various regimes. We show that, although in the experimental conditions explored so far the method is in fact inefficient, a suitable choice of initial temperatures and metals can lead to unexpectedly large cooling effect, even in the presence of dissipative phenomena. Our results suggest that this principle can be re-envisioned today as a performing refrigeration method to access the μK regime.

DOI: [10.1103/PhysRevB.80.024503](https://doi.org/10.1103/PhysRevB.80.024503)

PACS number(s): 07.20.Mc, 05.70.-a, 74.25.Bt

I. INTRODUCTION

Since the very early discovery of the laws of thermodynamics, cooling represents one of the most fascinating challenges for both experimental and theoretical physics.^{1,2} A well known cryogenic principle is the adiabatic demagnetization, based on the property that ordinary magnetic materials, such as paramagnetic salts, experience an entropy decrease when a magnetic field is applied due to the alignment of their atomic dipoles. This effect is currently applied also to nuclear spins under large magnetic fields, allowing reaching of the μK regime in nuclear demagnetization refrigerators.¹

In superconducting materials, however, the opposite cooling principle is observed. It is well known³ that a sufficiently strong magnetic field drives a superconductor (S) into the normal (N) state and that such phase transition occurs with a supply of latent heat since the S state is a much more ordered phase than N at a given temperature. As a consequence, if a magnetic field with intensity H increasing from zero up to the critical value H_c is quasistatically applied on a thermally isolated superconductor, its entropy \mathcal{S} per unit volume is preserved,

$$\mathcal{S}^N(T_f, H = H_c) = \mathcal{S}^S(T_i, H = 0), \quad (1)$$

and the metal cools from the initial temperature T_i down to a final temperature T_f ,^{4,5} as illustrated in Fig. 1. This cryogenic principle, known after the pioneering works by Mendelssohn and Moore⁶ and by Keesom and Kok⁷ in 1934 as “adiabatic magnetization of a superconductor” (AMS), offers the advantage that the required magnetic fields are much lower ($H \ll 1$ T) than those typically used in adiabatic demagnetization refrigerators. Furthermore, the presence of a metal greatly simplifies the contacting to devices and allows faster equilibration time scales. Although the validity of AMS was successively confirmed by other experiments,^{8–10} only a relatively small cooling effect was observed so far: the temperature was lowered from 2.50 to 2.22 K on tin samples,^{6,11} from 1.43 to 1.32 K on thallium samples, and from 3.63 to

3.54 K on lead spheres.¹⁰ It, thus, never became of practical use as a cryogenic technique and its theoretical modeling has also been overlooked.¹² On the other hand, the exponential growth of nanotechnological applications at low temperature demands higher performance of refrigerators, which are required to be more versatile, faster, and not invasive. The aforementioned features of AMS seem quite promising to this purpose and a detailed analysis of this refrigeration principle is desirable.

Here we present a dynamical description of the adiabatic magnetization effect, taking into account the role of dissipative phenomena and computing both the final temperature and the process time scales. This analysis allows us to show that, while the conditions of the experiments carried out so far were not suitable for cooling, realistic regimes can be identified in which the adiabatic magnetization can be exploited as a performing cooling technique.

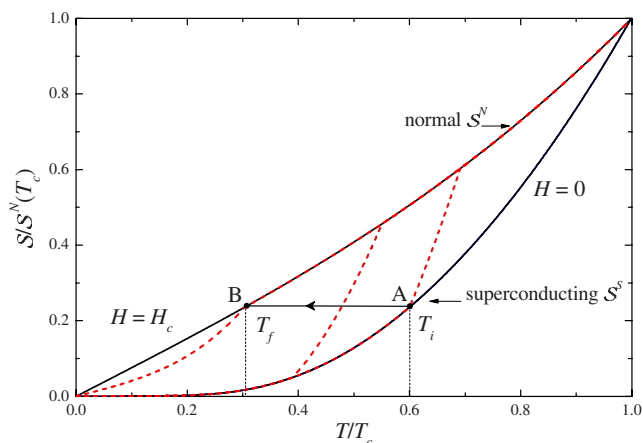


FIG. 1. (Color online) Adiabatic magnetization of a superconductor. Solid curves describe the entropy \mathcal{S} of a metal in the N state and in the S state as a function of the reduced temperature. When a magnetic field is applied on a thermally isolated superconductor at T_i , the metal is driven into the N state ($A \rightarrow B$) and the temperature decreases down to T_f . Dashed lines refer to the entropy in the intermediate state.

II. DESCRIPTION OF THE SYSTEM

We consider the case of type-I superconductors and start our analysis with some remarks about thermodynamics. In each phase the entropy includes a phonon and an electronic contribution, $\mathcal{S}^{N/S} = \mathcal{S}_{ph} + \mathcal{S}_{el}^{N/S}$. Explicitly, $\mathcal{S}_{ph}(T) = \alpha T^3$, where T is the temperature and α is the coefficient related to the Debye temperature. The electronic entropy in the N state has a linear behavior $\mathcal{S}_{el}^N(T) = \gamma T$. The contribution of spin paramagnetism is negligible in the range of magnetic fields we are interested in, $H \ll 1$ T, so that $\mathcal{S}^N(T, H_c) \cong \mathcal{S}^N(T, 0)$. In the S phase the condensate is a coherent state with vanishing entropy so that \mathcal{S}_{el}^S is purely due to quasiparticles and can be obtained from the BCS theory as

$$\mathcal{S}_{el}^S(T) = -2\nu_F k_B \int_{-\infty}^{\infty} dE \mathcal{N}(E, T) f(E) \ln[f(E)], \quad (2)$$

where ν_F is the normal density of states (DOS) at the Fermi level, $f(E) = [1 + \exp(E/k_B T)]^{-1}$ is the Fermi-Dirac distribution function, and $\mathcal{N}(E, T) = |E| / \sqrt{E^2 - \Delta(T)^2} \Theta[E^2 - \Delta(T)^2]$ is the BCS normalized DOS, with $\Delta(T)$ denoting the superconducting order parameter and $\Theta(x)$ the Heaviside function.

For a given initial temperature T_i , the final temperature T_f of the metal is determined by Eq. (1), which can be rewritten as

$$T_f + \frac{T_f^3}{(T^*)^2} = \frac{T_i^3}{(T^*)^2} \left[1 + \left(\frac{T^*}{T_c} \right)^2 \Phi \left(\frac{T_i}{T_c} \right) \right], \quad (3)$$

indicating that T_f depends, in general, on *two* characteristic parameters, namely, the critical temperature T_c of the superconductor and

$$T^* \doteq \sqrt{\gamma/\alpha} = \sqrt{5ZT_D^3/8\pi^2 T_F}, \quad (4)$$

which defines the temperature below which the entropy of the N state is dominated by the electron contribution. Here, Z denotes the nominal valence while T_F and T_D denote the Fermi and Debye temperatures of the metal, respectively. Furthermore, Φ is a universal function of T/T_c , defined through the relation $\mathcal{S}_{el}^S(T)/\mathcal{S}_{ph}(T) = (T^*/T_c)^2 \Phi(T/T_c)$, which is exponentially small for $T/T_c < 0.1$, and of the order of unity for $0.5 \leq T/T_c \leq 1$. Despite the simplicity of its derivation, Eq. (3) contains important physical insight. Indeed if the initial temperature T_i is of the same order as T^* , then so is the final temperature T_f ($T_f \lesssim T_i$), even if $T_i \ll T_c$. In this regime the AMS is therefore clearly inefficient as a cooling mechanism. By contrast, if $T_i \ll T^*$, the final temperature decreases as

$$T_f \approx T_i^3 / (T^*)^2. \quad (5)$$

This *cubic* dependence stems from the fact that, in this temperature regime, the AMS effectively transforms the entropy of phonons into the entropy of electrons. We emphasize that this effect represents an advantage with respect to the *linear* gain factor T_f/T_i characterizing the adiabatic demagnetization process.¹ The efficiency of the AMS thus heavily depends on the material choice and on the initial temperature range.

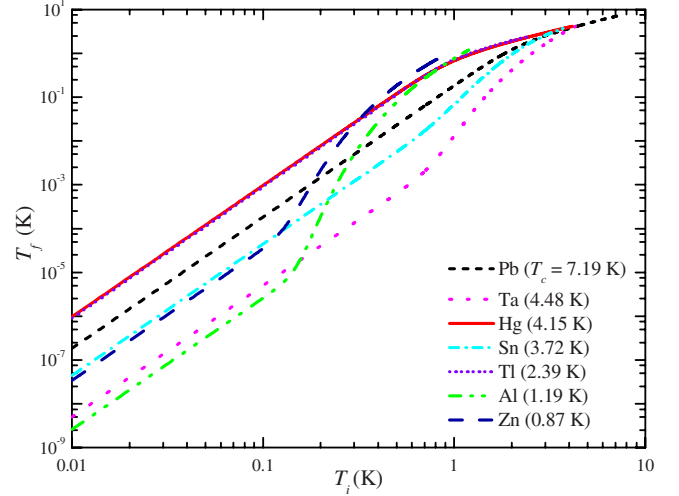


FIG. 2. (Color online) Final temperature T_f vs initial temperature T_i for several type-I superconductors in the absence of dissipative effects.

Figure 2 shows T_f vs T_i calculated for several superconductors from 10 mK to the zero-field critical temperature T_c . The low-temperature linear behavior in the log-log plot accounts for the cubic dependence [Eq. (5)] and occurs in all materials. At higher temperatures, differences emerge between metals that exhibit $T^* < T_c$ (such as Pb, Hg, and Tl) and those with $T^* > T_c$ (such as Al, Zn, and Ta). In the former case $T_f \lesssim T_i$, whereas in the latter case T_f exhibits a steep decrease governed by T_c , i.e., $T_f \approx T_i^3 \Phi(T_i/T_c) / T_c^2$, before the crossover to the cubic law [Eq. (5)]. It is noteworthy that most experiments were concerned with the first group of metals and with $T_i \sim T^*$. This explains the unsatisfactory cooling observed on Sn (Refs. 6 and 11) and Pb.¹⁰ Our analysis suggests that tantalum (Ta) is a good candidate since $T^*/T_c \gtrsim 3$, and it allows us to obtain T_f in the range $\sim \mu\text{K} - \text{mK}$ starting from T_i in the range $\sim 100 \text{ mK} - 1 \text{ K}$. Notice that Sn is suitable only if $T_i \leq 0.6 \text{ K}$, whereas Al is even better for $T_i \leq 0.2 \text{ K}$.

So far, using purely thermodynamical arguments and BCS theory, we have shown that AMS may, in principle, lead to extremely low values of T_f , provided the superconducting metal and initial temperature are appropriately chosen. However, the influence of dissipative effects must be taken into account in order for such a method to be considered as a promising cooling technique. First of all, when a magnetic field is applied to a type-I superconductor, the transition to the N phase is preceded by formation of an intermediate state (IS), where S and N phases coexist for $H_c'(T) < H < H_c(T)$. Here $H_c'(T) = (1-n)H_c(T)$, n is the demagnetization factor, $H_c(T)$ is the critical field defined through the relation $dH_c^2(T)/dT = (2/\mu_0)[\mathcal{S}^S(T, 0) - \mathcal{S}^N(T, 0)]$,⁴ and μ_0 is the vacuum permeability. The presence of a normal fraction x_N in the IS yields dissipative eddy currents when the magnetic field is increased with time. Furthermore, in a cryostat the superconductor is connected to some mounting support that remains at the initial temperature T_i ; the metal is thus exposed to a heat flux, which cannot be neglected in view of its relatively small low-temperature specific heat. Finally, once

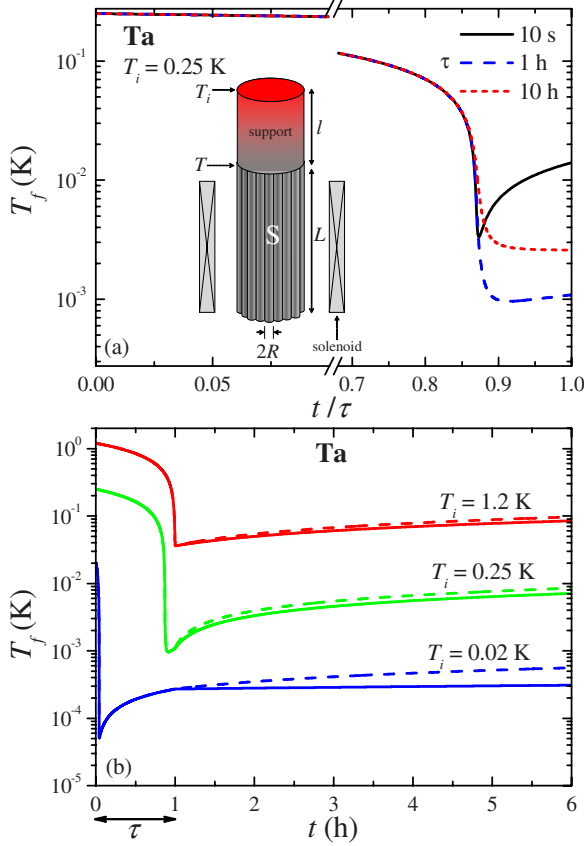


FIG. 3. (Color online) (a) Time evolution of T_f in the intermediate state calculated at $T_i=250$ mK for three values of τ . The inset shows a scheme of the adiabatic magnetization cooler. (b) Full time evolution of T_f calculated at three different T_i for $\tau=1$ h. Dashed curves refer to $P_{load} \neq 0$: from bottom to top, $P_{load}=10$ pW, 1 nW, and 100 nW. All calculations were performed for Ta (see text).

the cooling is realized, heating generated by measurements on any device attached to the cryostat has to be considered. Thus, even assuming that the range of initial temperatures and the superconductor are properly chosen, the existence of dissipative effects leads to the following questions: (i) is the AMS-based cooling robust against these effects? (ii) if so, what are the typical time scales in which low temperatures are reached, and how long can these be maintained?

To address these questions, we have analyzed the AMS *dynamically*, i.e., the process is governed by the equation $\partial_t S = P(t)/T(t)$, where P is the total dissipated power per unit volume that involves the three contributions mentioned above. For simplicity, we consider a bundle of N_w long and thin superconducting wires of radius R and length L each, attached to an insulating support of length l , as sketched in the inset of Fig. 3(a). The AMS is driven by the magnetic field and three time regimes can be distinguished. In the first one the magnetic field is increased from zero to $H'_c(T_i)$, and no cooling occurs since the whole system remains superconducting so that $P=0$ and $T=T_i$. In the second regime (cool down), H is varied from $H'_c(T_i)$ up to $H_c(0)$ over a time τ and the system enters into the IS state. While a detailed description of the IS for a given geometry is, in general, quite complicated, our purpose is to capture its main physical charac-

teristics. We shall thus follow Ref. 5 and assume that the N and S regions of the IS are uniformly distributed so that the normal fraction x_N increases with the magnetic field as $x_N(T, H) = 1 - n^{-1}(1 - H/H_c(T))$, and that the entropy is a linear combination of the N and S entropies, $S(T, H) = x_N S^N(T, 0) + (1 - x_N) S^S(T, 0)$. In this case the AMS is described by the differential equation

$$C_V(T, H) \dot{T} - \frac{\mu_0}{n} T \frac{dH_c(T)}{dT} \dot{H} = P, \quad (6)$$

where

$$C_V(T, H) = x_N C_V^N(T) + (1 - x_N) C_V^S(T) + C_V^{lat}(T, H) \quad (7)$$

is the total specific heat (per unit volume) in the IS, $C_V^{N/S}(T) = T \partial S^{N/S}(T) / \partial T$, and

$$C_V^{lat} = [TH / \mu_0 n H_c^3(T)] [S^N(T, 0) - S^S(T, 0)]^2 \quad (8)$$

is the contribution from the latent heat. As soon as $x_N \neq 0$, the cooling mechanism is enabled and the temperature of the metal starts to lower, although contrasted by the dissipative effects. A simple calculation shows that the variation in the magnetic field $B = x_N \mu_0 H_c(T)$ trapped in the normal fraction induces eddy current dissipation

$$P_{eddy}(t) = R^2 \sigma \dot{B}^2 / 8 \quad (9)$$

in each wire, where σ is the electric conductivity of the metal. At the same time, the temperature gradient across the insulating support between the “hot” upper surface at temperature T_i and the “cold” lower surface in contact with the metal [see the inset of Fig. 3(a)] leads to a heat flow

$$P_{supp} = b(T_i^{\beta+1} - T^{\beta+1}) / (\beta + 1) l L. \quad (10)$$

Here, b and β are parameters characterizing the temperature dependence of thermal conductivity $\kappa_{supp}(T) = bT^\beta$ of the insulating support.¹ Any temperature gradient in the metal has been neglected due to its relatively high thermal conductivity.

III. RESULTS

We present now the results concerning the temperature evolution as a function of time in AMS. Figure 3(a) displays the behavior of temperature for $0 \leq t \leq \tau$ calculated for three values of τ , starting from $T_i=0.25$ K. For simplicity we assumed H to vary linearly with time. For $t \ll \tau$, the temperature experiences a relatively slow decrease, whereas a fast drop is observed for $t \lesssim \tau$. The cooling effect is eventually contrasted by both dissipative eddy currents and heat flow from the support. It is worth emphasizing that P_{eddy} and P_{supp} behave differently with respect to the velocity of the magnetic-field variation. For fast field variations [solid curve of Fig. 3(a)] P_{eddy} is relevant and P_{supp} is suppressed. In contrast, for slow field variations [dotted curve of Fig. 3(a)] Joule heating has a minor effect while the heat flow from support affects the cooling for a longer time. For a given geometry and initial temperature, the competition of these two terms determines the optimal time scale that allows

reaching of the lowest temperature, as shown by the dashed curve in Fig. 3(a) for $\tau=1$ h. Such time scale depends on the electric conductivity of the metal and the thermal conductivity of the support. Tantalum seems to be a good candidate superconductor due to its relatively low conductivity $\sigma \sim 10^9 \Omega^{-1} \text{m}^{-1}$ and high specific heat ($\gamma \sim 523 \text{Jm}^{-3} \text{K}^{-2}$ and $\alpha \sim 2.63 \text{Jm}^{-3} \text{K}^{-4}$). We note that aluminum (Al), in spite of its high ratio T^*/T_c , is less suitable for AMS due to its extremely high electric conductivity; alternatively, tin (Sn) may be a fair choice. As far as the support is concerned, a good insulator such as polyvinyl chloride (PVC), with parameters $b=1.8 \times 10^{-5} \text{Wm}^{-1} \text{K}^{-1}$ and $\beta=2.05$ (see Ref. 1), seems appropriate. The plots of Fig. 3 refer to this case.¹³

The last time regime corresponds to the case where the system is fully normal. The magnetic field is not further varied [$H \equiv H_c(0)$] so that $P_{\text{eddy}}=0$. This is the regime where measurements are typically carried out on a device thermally anchored to the metal. We have thus included a constant load power for $t > \tau$ arising from the measurement (P_{load}) besides P_{supp} . The result of the whole dynamical process is shown in Fig. 3(b) for three initial temperatures T_i , corresponding to the base temperature of a ⁴He cryostat ($T_i=1.2$ K), a ³He cryostat ($T_i=250$ mK), and a dilution refrigerator ($T_i=20$ mK). For each T_i , the solid (dashed) curve represents the temperature evolution without (with) P_{load} . Notably, this cooling method ensures in all these ranges of operation a temperature gain of about two orders of magnitude, which can be reached within an hour or less and can be maintained for several hours. This represents an advantage with respect to the time scales typical of the adiabatic demagnetization of nuclei. The external load sustained by the AMS method depends on the temperature range of operation. For instance, we have calculated that a bundle of wires of about $4 \times 10^3 \text{cm}^3$ volume operating at $T_i=1.2$ K can sustain a power load of 100 nW without significantly affecting its final temperature, whereas at $T_i=20$ mK a power load of 10 pW increases T_f of few hundreds of μK after 5 h of operation [see Fig. 3(b)]. We stress that ordinary superconducting electronics (such as tunnel-junctions circuits, radiation detectors, and superconducting quantum interference devices) as well as single-electron devices exhibit power dissipation typically below 1 pW, thus suggesting that AMS is suitable to operate on nanostructures in the ultralow-temperature regime.

Finally we notice that, since the magnetization must evolve through equilibrium states, the variation in the ap-

plied magnetic field must proceed slowly enough for relaxation processes to ensure equilibrium between electrons and lattice phonons. The determination of such time scales in the IS is a crucial issue since the N and S phases have much different characteristic relaxation rates.¹⁴ Analyzing the three terms of Eq. (7), one can easily prove that even a small normal fraction $x_N \sim 10^{-3}$ is sufficient for C_V^N to largely dominate the other two contributions. Thus, apart from an extremely small range of magnetic fields, the specific heat of the superconductor in the IS is essentially determined by the electronic contribution in the N fraction, which drives the cooling, “dragging” the lattice phonons and the S fraction. An upper bound for the relaxation time characterizing the process is therefore represented by the inverse of the electron-phonon scattering rate in the N phase, which scales as $\tau_{\text{el-ph}}^{-1} \propto T^3$ (see Ref. 2), and is typically much shorter than that of the superconducting phase. For Ta in the temperature range $2 \times 10^{-4} - 5 \times 10^{-1}$ K, $\tau_{\text{el-ph}}$ lies in the range $\sim 10^{-7} - 10^3$ s,¹⁴ thus ensuring the consistency of our quasi-static approach.

IV. CONCLUSIONS

In conclusion, we have provided a dynamic description of cooling by adiabatic magnetization of superconductors. We have shown that, while in the experimental conditions explored so far the method is in fact inefficient, a suitable choice of temperature ranges and superconductors make this principle promising as a high-performance refrigeration technique. Besides involving low magnetic fields (i.e., $\sim 10^{-2} - 10^{-1}$ T), the present method offers the additional advantage that the final temperature depends cubically on the initial one [see Eq. (5)]. Moreover, we find that the cool-down times are comparable or shorter than those of typical demagnetization cryostats in the same temperature range while the warming-up rates can be on the order of several hours under continuous power load (see Fig. 3). Our results suggest that magnetization cycles to improve this cooling principle can also be envisioned.

ACKNOWLEDGMENTS

We acknowledge R. Fazio and J. P. Pekola for fruitful discussions, and the NanoSciERA “NanoFridge” EU project and “Rientro dei Cervelli” MIUR program for financial support.

*f.dolcini@sns.it

†f.giazotto@sns.it

¹F. Pobell, *Matter and Methods at Low Temperatures*, 3rd ed. (Springer, Berlin, 2007).

²See, e.g., F. Giazotto, T. T. Heikkilä, A. Luukanen, A. M. Savin, and J. P. Pekola, *Rev. Mod. Phys.* **78**, 217 (2006), and references therein.

³See, e.g., G. Ryckayzen, *Theory of Superconductivity* (John Wiley & Sons, New York, 1965).

⁴D. Shoenberg, *Superconductivity* (Cambridge University Press, Cambridge, 1965).

⁵A. C. Rose-Innes and E. H. Rhoderick, *Introduction to Superconductivity* (Pergamon Press, Oxford, 1969).

⁶K. Mendelssohn and J. R. Moore, *Nature (London)* **133**, 413 (1934).

⁷W. H. Keesom and J. A. Kok, *Physica (Amsterdam)* **1**, 595 (1934).

⁸W. H. Keesom and P. H. van Laer, *Physica (Amsterdam)* **4**, 487

- (1937).
- ⁹J. G. Daunt and K. Mendelssohn, Proc. R. Soc. London **160**, 127 (1937); J. G. Daunt, A. Horseman, and K. Mendelssohn, Philos. Mag. **27**, 754 (1939).
- ¹⁰R. L. Dolecek, Phys. Rev. **94**, 540 (1954); **96**, 25 (1954).
- ¹¹M. Yaqub, Cryogenics **1**, 101 (1960); **1**, 135 (1961).
- ¹²K. Mendelssohn, Nature (London) **169**, 366 (1952).
- ¹³In addition we set $T_c=4.48$ K, $R=5 \times 10^{-4}$ m, $n=5 \times 10^{-4}$, $l=0.3$ m, $L=0.4$ m, and $N_w=10^4$.
- ¹⁴S. B. Kaplan, C. C. Chi, D. N. Langenberg, J. J. Chang, S. Jafarey, and D. J. Scalapino, Phys. Rev. B **14**, 4854 (1976).